

Interaction Between Hysteresis Controlled Inverters used in Distributed Generation Systems

M. Milošević, J. Allmeling, G. Andersson

EEH Power Systems Laboratory Swiss Federal Institute of Technology (ETH Zurich)

milosevic@eeh.ee.ethz.ch, allmeling@eeh.ee.ethz.ch, andersson@eeh.ee.ethz.ch

Abstract—Many new primary energy sources in distributed generation systems are interfaced with the electric grid through power electronic inverters. If several of these are present in proximity of each other, interactions between them could arise. This paper presents a study of the interaction between hysteresis controlled voltage source inverters connected to the same power network. The coupling between the inverters results in an interdependence of their switchings. It is shown that this interdependence is not detrimental, and a reduction of the ripple in the resulting current supplied to the network as compared to the single inverter case is obtained. The effects of various parameters of the inverters are analyzed.

I. INTRODUCTION

In the last few years, the use of renewable energy sources has become popular in many parts of the world. Renewable sources of energy can be divided into two groups: 1) small scale renewable sources which are connected to the power distribution network (located close to the customers) and 2) large-scale renewable sources which are located far away from the customers where renewable energy is available in large quantities.

Fuel cells and solar cells belong mostly to group 1 above, generate DC voltage and current. Therefore, systems containing these cells often require a power electronics interface for power conditioning. The interface usually consists of a converter system converting a DC voltage or an ac voltage of varying frequency to an ac voltage of system frequency.

A large number of grid-connected renewable generators are potentially able to cause harmonic problems. Adverse interactions between several interfaces could arise in the network. It is thus clear that interface models for the connection between the network and the energy source are needed in order to examine possible interactions between several interfaces regarding current harmonics.

Voltage source inverters are described in detail in [1]. An inverter has to shape the current into a sinusoidal waveform in order to feed energy from a renewable energy source into the utility grid. On the other hand, the inverters themselves are sensitive to harmonic currents and may operate incorrectly as a result of harmonic current distortion [2].

With this in view, various standards and recommendations like the IEEE-519 [3] are being revised to limit the harmonics that any system can inject into the grid. To meet such standards, it is important that the interface with the grid draws a current as sinusoidal as possible.

Recently, the use of parallel operating systems is becoming

common in various applications, such as new energy systems with renewable energy sources [4]. Parallel operation of voltage source inverters with other inverters, or with the utility source is sensitive to disturbances from the load or other sources [5].

The interaction between several power electronics systems integrated in a power system is a new topic. The inverters can be quite close to each other, and it is not excluded that interactions of adverse nature could occur. The control strategy of the inverters has a strong influence on the interaction between parallel connected inverters [5].

A schematic overview of a power system with renewable sources of energy is given in Fig. 1. The system consists of a number of generators (power sources) (G) where electricity is generated from renewable sources of energy. The generators may be connected directly to the electricity network or through some kind of interface (IF).

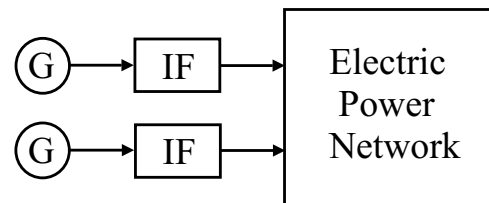


Fig. 1. Schematic presentation of renewable energy sources connected through the interface to the power network

This paper presents the theoretical analysis and simulation results of the interface consisting of parallel inverters, which reduces the distortion in the current supplied to the power network. The primary considerations for such an interface for renewable energy sources is minimum ripple in the current fed into the network. This work presents an analysis of multi-inverter single phase systems. So far no detailed method for the analysis of multi-inverter interactions with respect to the current harmonics has been reported in the literature.

In the analyzed parallel inverter system, all of the modules have the same configuration, and each module includes its inner hysteresis current control loop as described in the following.

The rest of the paper is organized as follows - the system description is given in Section II, followed by the description of the simulation model in Section III. The simulation results

are presented in Section IV, followed by conclusions in Section V.

II. SYSTEM DESCRIPTION

A. Hysteresis Current Control

The current control method applied here is the hysteresis control method [2]. With this control method the switching of the inverters does not only depend on an external control signal but also on the momentary currents in the circuit. The resulting interactions between the parallel connected inverters will be examined when this control method is applied.

The main idea of this type of current control is that the switching action is performed each time the current error reaches the limits of the hysteresis band defined in advance. The average switching frequency depends on the width of the hysteresis band. When the hysteresis bandwidth is small the switching frequency is high (because the current changes fast from the upper limit to the lower and vice versa), which means also, that dominant current harmonics are of higher order. The switching period increases (i.e. switching frequency decreases) with increasing hysteresis bandwidth. Due to the nonlinearities in the hysteresis control method, its behavior is analyzed by means of time domain simulations.

The current control loop is shown in Fig.2.

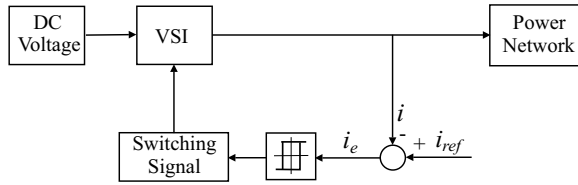


Fig. 2. Basic principle of inverter hysteresis current control method

The reference current i_{ref} subtracts the inductance current i giving the error current i_e , which goes through the hysteresis controller to obtain signals for switching full bridge inverters. The inverters are controlled with individual controllers.

B. Model of the Circuit

The interface model consists of full bridge voltage source inverters (VSI) connected in parallel to the same power network, see Fig. 3. The power network is modelled with the inductance L_n and the inner voltage u_L . The supplying DC voltages U_{dc1} and U_{dc2} are the voltage outputs of renewable sources of energy.

The coupling of the inverters is defined by the coupling factor k :

$$k = \frac{L_n}{L_n + L_1 + L_2}, \quad 0 \leq k < 1 \quad (1)$$

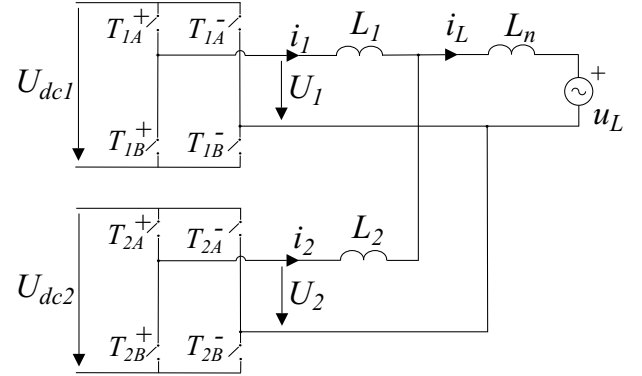


Fig. 3. The model of the renewable energy source interface system (two parallel connected VSIs)

When $k = 0$ it implies $L_n = 0$, which means that inverters are not coupled.

In general, if the network inductance $L_n \ll L_1, L_2$ there is no coupling between inverters. On the other hand, if $L_n \gg L_1, L_2$ there is a strong coupling between the inverter currents i_1 and i_2 .

In a real system, it is desirable to have the coupling factor as small as possible. However, in this paper the general case for different values of k is analyzed in order to examine what is the interaction between coupled inverters with respect to the current harmonics if the inverters are being connected to the same power network.

A similar problem was investigated in [6], where the authors analyzed the parallel connected single phase hysteresis controlled boost converters with respect to the reduction of the input current ripple with constant switching frequency of the individual systems.

Assuming ideal symmetry of both systems ($U_{dc1} = U_{dc2} = U_{dc}$, $L_1 = L_2 = L$), the mathematical equations of the system are given by:

$$U_1 = (L + L_n) \frac{di_1}{dt} + L_n \frac{di_2}{dt} + u_L \quad (2)$$

$$U_2 = L_n \frac{di_1}{dt} + (L + L_n) \frac{di_2}{dt} + u_L \quad (3)$$

The two possible inverter switching states can be defined as:

1) State "zero" $s_{1(2)} = 0$ when the switches $T_{1(2)B}^+$ and $T_{1(2)A}^-$ are closed (Fig. 4);

2) State "one" $s_{1(2)} = 1$ when the switches $T_{1(2)A}^+$ and $T_{1(2)B}^-$ are closed (Fig. 5)

(s_1 corresponds to the first inverter and s_2 corresponds to the second inverter).

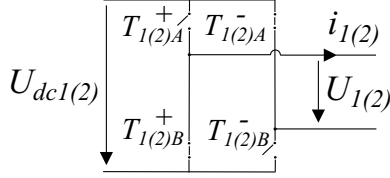


Fig. 4. The switching positions for the state "zero" ($s = 0$)

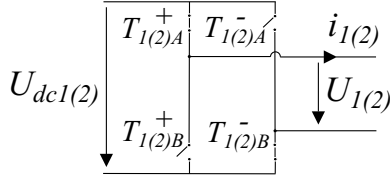


Fig. 5. The switching positions for the state "one" ($s = 1$)

The current derivatives (di_1/dt and di_2/dt) depend on four possible different positions of the inverter switches:

$$1) s_1 = 0, s_2 = 0 (U_1 = -U_{dc}, U_2 = -U_{dc})$$

$$\frac{di_1}{dt} = \frac{di_2}{dt} = -\frac{U_{dc} + u_L}{2L_n + L} = m_0 \quad (4)$$

$$2) s_1 = 0, s_2 = 1 (U_1 = -U_{dc}, U_2 = U_{dc})$$

$$\frac{di_1}{dt} = -\frac{U_{dc}}{L} - \frac{u_L}{2L_n + L} = m_1 \quad (5)$$

$$\frac{di_2}{dt} = \frac{U_{dc}}{L} - \frac{u_L}{2L_n + L} = m_2 \quad (6)$$

$$3) s_1 = 1, s_2 = 0 (U_1 = U_{dc}, U_2 = -U_{dc})$$

$$\frac{di_1}{dt} = m_2; \frac{di_2}{dt} = m_1 \quad (7)$$

$$4) s_1 = 1, s_2 = 1 (U_1 = U_{dc}, U_2 = U_{dc})$$

$$\frac{di_1}{dt} = \frac{di_2}{dt} = \frac{U_{dc} - u_L}{2L_n + L} = m_3 \quad (8)$$

The rate of the current changes for both inverters is influenced by each switching state (s_1 and s_2) of both inverters. The states s_1 and s_2 can take values 0 or 1, which means that when $s_1 = 0$ the current i_1 decreases and when $s_1 = 1$ it

increases. The same applies to the state s_2 and the current i_2 .

It can be seen that there exist identical current changing rates for state combinations $s_1 = 0, s_2 = 1$ and $s_1 = 1, s_2 = 0$. Therefore, there is a symmetry in the current shapes (Fig. 6). The shape of i_1 related to the lower hysteresis bandwidth and the shape of i_2 related to the upper hysteresis bandwidth show the symmetry conditions. The switching frequency depends on how fast the current changes from the upper limit to the lower limit and vice versa. Also, the switching interval does not remain constant during the simulation but varies along with the current waveform, so that there is a "trapezoidal" shape of the current harmonics.

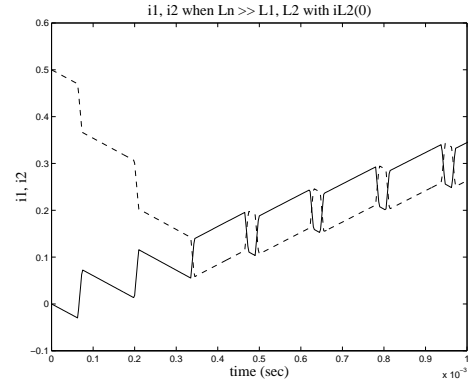


Fig. 6. The line current mutual coupling (i_1 (solid) and i_2 (dashed)) when $L_n \gg L_1, L_2$ ($k \approx 1$) with the initial current in L_2 (i_2 is offset)

For the case when $k > 0$ the current interdependence can be noticed. Inverter switching of the systems depends on each other, which means that when the current error of one inverter touches the border of its hysteresis bandwidth the current in another inverter changes direction and vice versa (Fig. 6).

III. SIMULATION MODEL

The assumption of identical components for both VSIs leads to the expectation that there is no phase shift between the currents i_1 and i_2 and no staggered switching frequency of the individual systems. The switching phase shift that exists in the beginning is maintained during the simulation. This assumption is confirmed with the simulation model for the case when all parameters for both inverters are the same.

In real systems, parallel operating inverters are sensitive to disturbances from the load or from the other inverter. Therefore, to investigate the real system behavior, regarding the total harmonic distortion (THD) of the current, the following parameters are varied:

- 1) the initial line currents injected into the system;
- 2) the DC voltages supplying the partial systems;
- 3) the tolerance bandwidth for hysteresis current control;
- 4) the values of the inductances L_1 and L_2 as well as the value of the network inductance L_n , i.e. the coupling factor k .

By varying the initial current in the second inverter identical

switching of the inverters is avoided, but the switching phase shift that exists in the beginning remains during the simulation if the same parameters are used in both inverters. The result shows the switching phase shift of the line currents (i_1 and i_2), which leads to different switching frequencies of the inverters, but to smaller THD of the i_L compared to the THD of the i_1 and i_2 due to the harmonics phase shift and consequently to harmonic cancellations. The initial current in one of the decoupled inverters does not influence the mutual coupling, which implies that they still operate independently of each other.

Similar behavior of the system is obtained with the different DC voltages (Fig. 7). Therefore, this case is not presented in detail.

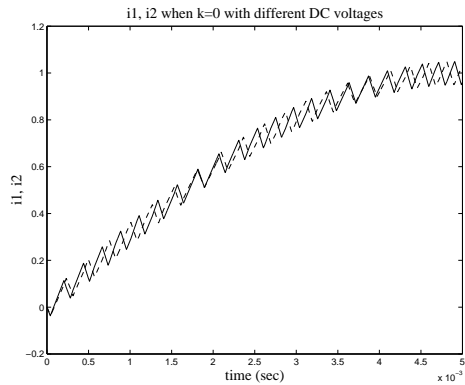


Fig. 7. The line currents i_1 (solid) and i_2 (dashed) with the different DC voltages with $k = 0$

If different hysteresis bandwidths are set for the individual systems, one can assume that it would be almost the same operating behavior of the whole system as if they were equal. However, there are basic differences in the operating behavior of the individual inverters. The switching phase-shift is not constant during the simulations anymore, as can be seen in Fig. 8.

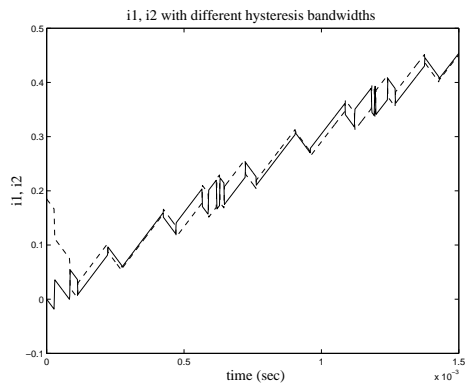


Fig. 8. The line currents i_1 (solid) and i_2 (dashed) with the different tolerance bandwidths for two hysteresis current controllers

With the unsymmetry of the systems due to slightly

different DC voltages ($U_{dc1} \neq U_{dc2}$) or slightly different inductances ($L_1 \neq L_2$) the whole system behaves similar to the case with different hysteresis bandwidths. In this paper, only the unsymmetry of the system behavior due to the different hysteresis bandwidths is presented. The effects of changing other parameters influence the mutual operation of the inverters in the same way.

IV. SIMULATION RESULTS

Simulations are done using both the SIMULINK and PLECS [7] in order to analyze the THD of the line currents as well as the THD of the current supplied to the network. The results are shown only for the variation of the system disturbance simulated by different initial currents $i_{L2}(0)$ of the inductance L_2 in the second inverter. The DC supplying voltages U_{dc1} and U_{dc2} and the magnitude of the inner voltage U_L are kept constant.

The THD is calculated as the average value over the last period of ten cycles of the simulations (to be sure that the system is in steady state). For example, the THD of i_1 calculated in the 9th period is 2.589% and in the 10th period is 2.587%. The THD is calculated using the formula:

$$THD = \frac{\sqrt{I^2 - (I_1)^2}}{I_1} \quad (9)$$

where, I is the rms value of the current and I_1 is the rms value of the fundamental frequency component of the current.

The simulation results for the THD with different values of the hysteresis bandwidth (h) are given in Fig. 9 (for the line current i_1) and in Fig. 10 (for the network current i_L) as a function of the initial current injected into the second inverter. All other parameters are the same for both inverters. The THD of i_2 is similar to the THD of i_1 .

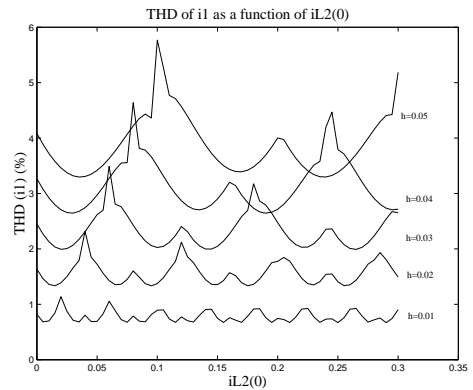


Fig. 9. The THD of the line current i_1 as a function of $i_{L2}(0)$ and different values of hysteresis bandwidth ($k \neq 0$)

From these figures, it can be seen that the THD changes periodically with $i_{L2}(0)$ and that the THD increases with

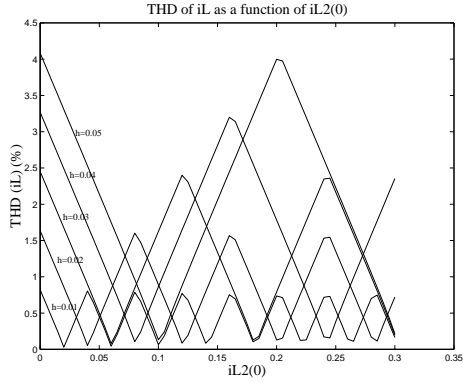


Fig. 10. The *THD* of the load current i_L as a function of $i_{L2}(0)$ and different values of hysteresis bandwidth ($k \neq 0$)

increasing tolerance bandwidth when all other parameters are the same and constant for both individual systems. It is understandable that the *THD* increases with the tolerance bandwidth, since the currents will then contain more high magnitude harmonics. However, it is interesting to find out why the current *THD* is sensitive to disturbances (in this case, the initial current in the second inverter) when the inverters are coupled.

Also, it can be noticed from Fig. 9 and Fig. 10 that, when the *THDs* of the line currents reach their maximum values, the *THD* of the network current reaches its minimum value. As well, for the minimum line *THD* values there is the average total *THD* value, and the local maximum values of the line *THD* implies the maximum value of the total *THD*.

The explanation for this is given in Fig. 11 and 12. The different "shape" of the mutual coupling between the inverter currents (for different initial currents) can be noticed. This explains the periodic dependence of the *THD* on the different initial currents since this "shape" periodically repeats with the initial current.

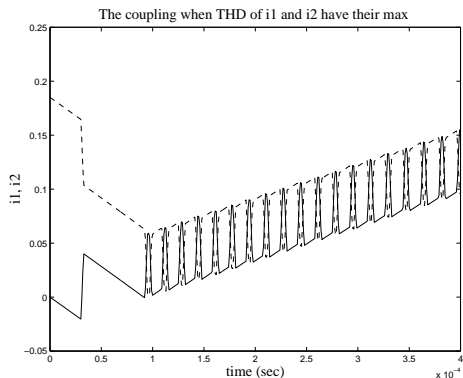


Fig. 11. The line currents i_1 (solid) and i_2 (dashed) when VSIs are coupled and when the line *THD* reaches its maximum value and the *THD* of the network current reaches its minimum value

The following step is to find out what parameters should be changed such that there is no *THD* dependence on the initial conditions of the system.

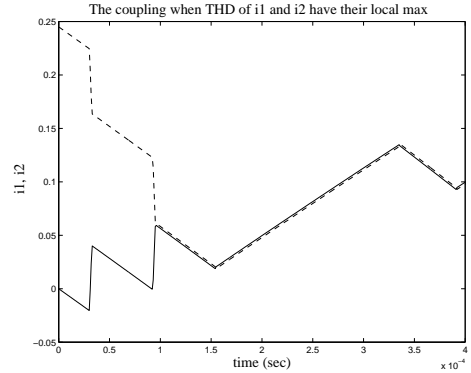


Fig. 12. The line currents i_1 (solid) and i_2 (dashed) when VSIs are coupled and when the line *THD* reaches its local maximum value and the *THD* of the network current reaches its maximum value

Having different hysteresis bandwidths leads to the *THD* independence of the initial currents (Fig.13).

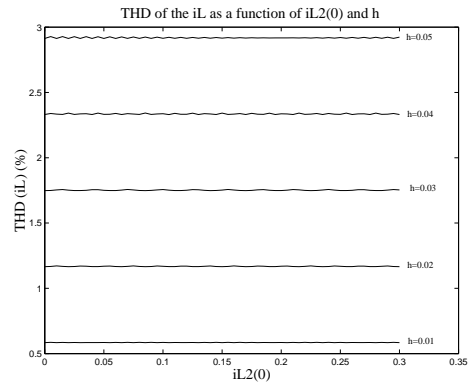


Fig. 13. The *THD* of total current as a function of the initial current with different hysteresis bandwidths

It is interesting to examine how the *THD* changes with the coupling factor k . The inductances L_1 and L_2 are kept constant and the inductance L_n is changed so that there are different levels of coupling. As L_n increases, the coupling factor k increases as well, which implies that there are two coupled VSIs. Having $k = 1$ implies that the sum of inductances L_1 and L_2 should be very small, i.e. the network inductance L_n should be very large, as can be seen in (1). This case is not of interest and therefore it is not analyzed here.

The simulation results for the single VSI and for two parallel connected VSIs supplying the same network are shown in Fig. 14. The upper diagram of this figure shows the *THD* of the current of the single inverter (i_1) supplying the network (dashed line) and the *THD* of the current of the same inverter (i_1) when the second VSI is parallel connected (solid line) to it. It can be seen that the *THD* of the single inverter current is lower when the second inverter is connected to it. This means that the harmonics of the current in the second inverter influence the current harmonics in the first inverter making the *THD* smaller. The second diagram shows the *THD* of the line current in the second inverter (i_2). The third diagram shows

the *THD* for current supplied to the network (i_L). For the case when there is a single VSI supplying the network, that current is actually the inverter current ($i_L = i_1$), and for the case when there are two parallel connected VSIs, that current is the sum of the inverter currents ($i_L = i_1 + i_2$). It can be seen that for the two parallel connected inverters, the current supplying the network has a smaller *THD* than the *THD* of the current of the single inverter supplying the network. This comparison of the *THD* values is possible due to the fact that the switching frequency of the system consisting of one inverter is higher than the switching frequency of the system with two inverters (the fourth diagram in Fig. 14).

The behavior of the interface consisting of three parallel connected inverters is analyzed, as well. The results show an even larger decrease of the *THD*.

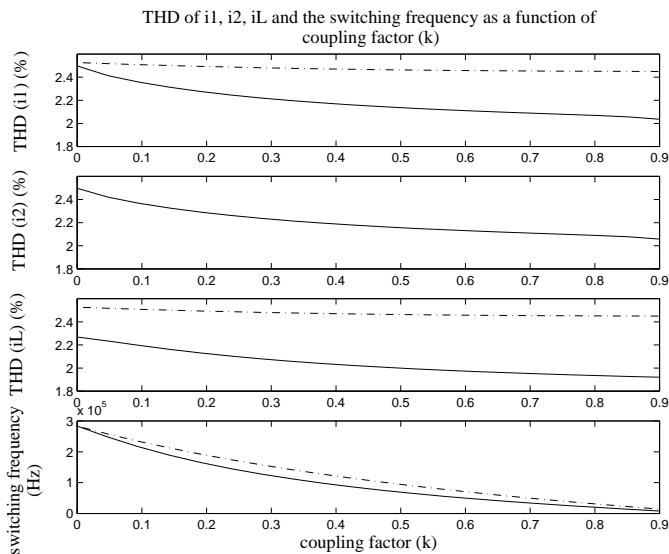


Fig. 14. The *THD* of the currents and the switching frequency as a function of the coupling factor (one VSI (dashed) and two VSIs (solid))

V. CONCLUSION

The unsymmetries of the parameters of the coupled inverters to the system behavior are analyzed with respect to the *THD* of the current supplied to the power network. The inverters exhibit a switching phase shift due to non identical parameters. The switching of the inverters is not independent of each other while they are coupled, although the hysteresis control applied separately to the individual systems maintains the same.

With the increase of the coupling between the partial systems the *THD* decreases. Also, the switching frequencies of the inverters decrease with the coupling, as well.

The *THD* of the current supplied to the network decreases with the number of parallel connected coupled inverters (interface) regardless of the nature of the supplied power network were the interfaces are connected to.

ACKNOWLEDGEMENT

Financial support from the Alliance of Global Sustainability (AGS) is gratefully acknowledged.

REFERENCES

- [1] N. Mohan, T.M. Undeland, W.P. Robbins, "Power Electronics, Converters, Applications and Design", John Wiley and Sons Inc. 1995
- [2] M. Meyer, A. Sonnenmoser, "A hysteresis current control for parallel connected line-side converters of an inverter locomotive" Fifth European Conference on Power Electronics and Applications, 1993, 13-16 Sep 1993, pp. 102-109, vol. 4
- [3] IEEE Recommended Practices and Requirements for Harmonic Control in Electric Power Systems, IEEE Standard 519, 1992
- [4] B. Lindgren, "Power-generation, Power-electronics and Power-Systems issues of Power Converters for Photovoltaic Applications", PhD Dissertation, Chalmers University of Technology, Göteborg, Sweden, 2002
- [5] T. Kawabata, S. Higashino, "Parallel operation of voltage source inverters", IEEE Transactions on Industry Applications, vol. 24, no. 2, Mar/Apr 1988, pp. 281-287
- [6] J.W. Kolar, G.R. Kamath, N. Mohan, F.C. Zach, "Self-adjusting input current ripple cancellation of coupled parallel connected hysteresis-controlled boost power factor correctors", 26th Annual IEEE Power Electronics Specialists Conference, 18-22 June 1995, vol. 1, pp. 164 - 173
- [7] J.H. Allmeling, W.P. Hammer, PLECS - Piece-wise linear electrical circuit simulation for Simulink, Proceedings of the International Conference on Power Electronics and Drive Systems, Hong Kong, July 1999, pp. 355-360

BIOGRAPHIES

Mirjana Milošević was born in Novi Sad, Serbia and Montenegro, in 1975. She received the Dipl.Ing. degree from the University of Novi Sad in 1999, and the MSc. Degree in 2002 from Northeastern University, Boston, MA, both in Electrical Engineering. Since 2002 she is PhD student and research assistant at the Power Systems Laboratory of Swiss Federal Institute of Technology (ETH) in Zurich.

Just Allmeling (S'98-M'03) was born in Hamburg, Germany, in 1972. He received his MS degree in electrical engineering from Aachen University, Germany, in 1996. In 2001 he received his PhD degree from the Swiss Federal Institute of Technology (ETH) in Zurich, where he is currently employed as a post-doctoral researcher. Dr. Allmeling is a co-founder of Plexim, a spin-off company from ETH Zurich, that develops software for the fast simulation of power electronic systems.

Göran Andersson (M'86, SM'91, F'97) was born in Malmö, Sweden. He obtained his M.S. and Ph.D. degree from the University of Lund in 1975 and 1980, respectively. In 1980 he joined ASEA:s, now ABB, HVDC division in Ludvika, Sweden, and in 1986 he was appointed full professor in electric power systems at the Royal Institute of Technology (KTH), Stockholm, Sweden. Since 2000 he is full professor in electric power systems at the Swiss Federal Institute of Technology (ETH), Zurich, where he heads the powers systems laboratory. His research interests are in power system analysis and control.